

Impact History of Eros: Craters and Boulders

Clark R. Chapman and William J. Merline

Southwest Research Institute, Suite 426, 1050 Walnut Street, Boulder Colorado 80302
E-mail: cchapman@boulder.swri.edu

Peter C. Thomas and Jonathan Joseph

Space Sciences Building, Cornell University, Ithaca, New York 14853

and

Andrew F. Cheng and Noam Izenberg

The Johns Hopkins University Applied Physics Laboratory, Laurel, Maryland 20723

Received January 26, 2001; revised May 21, 2001

Preliminary measurements of craters and boulders have been made in various locations on Eros from images acquired during the first nine months of NEAR Shoemaker's orbital mission, including the October 2000 low altitude flyover. (We offer some very preliminary, qualitative analysis of later LAF images and very high-resolution images obtained during NEAR's landing on 12 February 2001). Craters on Eros >100 m diameter closely resemble the saturated crater population of Ida; Eros is more heavily cratered than Gaspra but lacks the saturated giant craters of Mathilde. These craters and the other large-scale geological features were formed over a duration of very roughly 2 Gyr while Eros was in the main asteroid belt, between the time when its parent body was disrupted and Eros was injected into an Earth-approaching orbit (probably tens of Myr ago). Saturation equilibrium had been expected to shape Eros' crater population down to very small sizes, as on the lunar maria. However, craters <200 m diameter are instead progressively depleted toward smaller sizes and are a factor of ~200 below empirical saturation at diameters of 4 m. Conversely, boulders and positive relief features (PRFs) rise rapidly in numbers (differential power-law index ~ -5) and those <10 m in size dominate the landscape at high resolutions. The pervasive boulders and minimal craters on Eros is radically different from the lunar surface at similar scales. This may be partly explained by a major depletion of meter-scale projectiles in the asteroid belt (due to the Yarkovsky Effect: Bell 2001), which thus form few small craters and destroy few boulders. Additionally, the small size and low gravity of Eros may result in redistribution or loss of ejecta due to seismic shaking, thus preferentially destroying small craters formed in such regolith. Possibly Eros has only a patchy, thin regolith of mobile fines; the smaller PRFs may then reflect exposures of fractured bedrock or piles of large ejecta blocks, which might further inhibit formation of craters <10 m in size. Eros may well have been largely detached dynamically and collisionally from the main asteroid belt for the past tens of Myr, in which case its cratering rate would have dropped by two orders of magnitude, perhaps enhancing the relative efficacy

of other processes that would normally be negligible in competition with cratering. Such processes include thermal creep, electrostatic levitation and redistribution of fines, and space weathering (e.g., bombardment by micrometeorites and solar wind particles). Combined with other small-body responses to impact cratering (e.g., greater widespread distribution of bouldery ejecta), such processes may also help explain the unexpected small-scale character of geology on Eros. If there was a recent virtual hiatus in cratering of Eros (during which only craters <~300 m diameter would be expected to have formed), space weathering may have reached maturity, thus explaining Eros' remarkable spectral homogeneity compared with Ida. © 2002 Elsevier Science (USA)

Key Words: asteroids, Eros; cratering; impact processes; geological processes; surfaces, asteroids.

I. INTRODUCTION

Impact cratering is thought to have been the dominant process affecting the physical character of asteroids since early solar system epochs. Because of the comparatively small sizes and great distances of asteroids, research on asteroid impact history was largely limited to indirect inferences from meteorites until the first close-up images were obtained in the past decade. Studies of asteroid cratering address many issues, ranging from the origin of individual asteroids from catastrophic collisional disruption of parent bodies to the more practical issues of how human beings may interact with asteroid surfaces in the future (e.g., for scientific sample collection, mining of space resources, or hazard mitigation).

Until the NEAR Shoemaker spacecraft entered orbit around Eros in February 2000, the crater populations of only three asteroids had been studied at all closely—Ida and Gaspra by Galileo (Chapman *et al.* 1996a, 1996b) and Mathilde by NEAR

(Chapman *et al.* 1999). In addition, a few large craters have been recognized on other asteroids (e.g., HST images of Vesta, radar images of Toutatis); also the largest craters on Eros were imaged during NEAR's unintended 1998 flyby (Veverka *et al.* 1999). NEAR Shoemaker's year-long orbital mission, however, has provided an unprecedented opportunity to map craters over the whole surface of Eros down to sizes smaller than sampled in even the highest resolution Galileo images of Ida. Moreover, an October 2000 low altitude flyover (LAF) permitted the crater population to be sampled down to diameters of a few meters (Veverka *et al.* 2001). Even closer flyovers were made in late January 2001. Imaging during the final descent to the surface of Eros on 12 February 2001 resolved features in the landing locality as small as a couple of centimeters in size, approaching the scale that the Moon was imaged by the Surveyor landers.

At resolutions better than 50 m/pixel, images of planetary and satellite surfaces often reveal positive relief features (PRFs) including boulders. Seventeen such PRFs >40 m in size were recognized on portions of Ida (Lee *et al.* 1996), and boulders have been studied from high-resolution images of the Moon and the martian satellites (Lee *et al.* 1986; Morris *et al.* 1968). Now that NEAR Shoemaker has achieved unprecedented resolutions on Eros, we have found that boulders and other PRFs dominate the small-scale landscape of this body and that small craters are (unexpectedly) extremely rare. It is vital to inquire whether the unexpected nature of Eros' surface reflects generic processes affecting small, low-gravity bodies in general, or the environment in the asteroid belt, or instead is due to more particular attributes of Eros (e.g., its present location in Earth-approaching orbit).

The data and size-frequency statistics presented and interpreted here represent only a very small sampling of the craters and boulders that can eventually be studied from NEAR Shoemaker images. More comprehensive cratering statistics may be assembled in the future along with more thorough studies of other aspects of impact features on Eros. However, the preliminary data presented here already illustrate dramatic surprises about the impact record of Eros and justify first-order attempts at interpretation. (The work reported here is based on imaging available prior to submission of this paper in mid-January 2001. At the referees' suggestion, we now offer qualitative evaluation of what the latest LAF and landing images suggest about alternative interpretations.)

II. METHODOLOGY

The diameter-frequency statistics presented here are samplings of the crater and boulder populations on Eros. The population of largest craters on Eros is sampled from images taken during early high-altitude orbits, covering the majority of the northern hemisphere. The statistics of moderate-sized craters are derived from several smaller, representative regions imaged during later, lower orbits. Still smaller craters, as well as boulders and other PRFs, are assessed from images of still smaller localities acquired from 35 km orbits and from the October LAF. The locations of counted areas are listed in Table I.

In all cases, features are measured in sample/line coordinates for a minimum of six points around the crater rim or PRF periphery and are converted into average diameters by appropriate projection onto the current shape model (cf. Thomas *et al.* 2000)

TABLE I
Frames Measured for Craters and Boulders

Figure and symbol	Crater/boulder	Approx. lat/long (deg)	Frame/s
F1, large filled circle	C	N hemis. (large) ~10/~130 (moderate)	Many early images 127301410
F1, small filled circle	C	-40, 10/295, 355	130277015, 130275515, 130276951, 130277271, 130277207
F1, open square	C	8, 22/32, 40	132377227, 137746426
F1, open invert triangle	C	-2, 42/342, 18	132389462, 134951432, 132463256, 138667010, 138666948, 135533270, 137112830, 137112892, 132466952, 132465368
F1, open triangle	C	10/184	134185379, 134185655
F1, open diamond	C	10/189	137543929
F1, filled diamond	C	50/250	132926922
F2, small open circle (ref)	C	19/18	139479598
F1, large open circle	C	19/18	139479598
F2, small open circle (ref)	C	19/18	139479598
F2, large open circle	C	-26, 14	147953103, 147953078, 147953128
F2, filled diamond	B	-26/14	147953103, 147953078, 147953128
F2, filled square	B	10/184	134185379, 134185655
F2, filled triangle	B	17/35	137746426
F2, filled circle	B	19/18	139479598

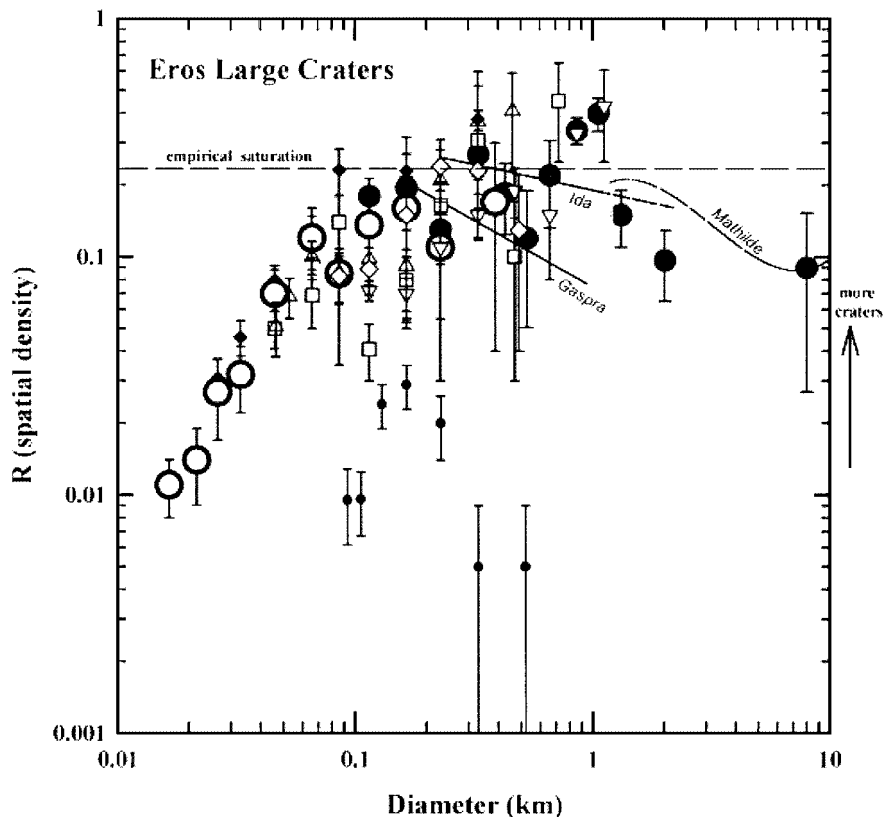


FIG. 1. This is an R-plot (differential size-frequencies divided by D^{-3} ; error bars reflect counting statistics only, not any systematic errors) showing the spatial densities of the larger craters on Eros. Craters larger than 200 meters diameter resemble the empirically saturated frequencies of craters on Ida; but smaller craters are deficient. In one region of Shoemaker Regio (small filled circles), crater densities are down by at least an order of magnitude. Different symbols represent different counting regions (see Table I).

using the “POINTS” software developed by J. Joseph. The raw measurements are saved in a file and can be reinterpreted as the shape model is refined. The aim of this project has been to develop preliminary statistics, so the measurements of individual features should not be considered definitive and are not presented here as an official catalog of craters or boulders. No attempt is made at this preliminary stage to classify the features into degradation states or to measure other physical parameters. However, we do attempt to achieve completeness—even for highly degraded features—down to some size limit (a multiple of the inherent resolution of the image), and counts deemed likely to be incomplete are omitted from the figures.

The measurements are presented (Figs. 1 and 2) on the standard R-plot (Crater Analysis Techniques Working Group 1979); error bars reflect \sqrt{N} counting statistics only. Areas of the counting surfaces were difficult to assess accurately during this project as the shape model was being refined, so systematic shifts of individual curves up and down by $\sim 30\%$ may eventually be required. We also have not yet completed a detailed analysis of other systematic errors in diameter measurements, especially for the smaller sizes in each data set, caused, for example, by the rectangular pixels of the MSI instrument. The measurements are assembled into diameter bins of variable width chosen to

have adequate statistics when feasible. In the R-plot, numbers per bin are divided by the incremental bin width ΔD , by the surface area, and by D^{-3} , where D is the median diameter of craters in the bin. The R-plot, therefore, presents the differential size-frequency relationship relative to $N \sim D^{-3}$, which is shown as a horizontal line on the log-log plot. It has the property that low spatial densities of features of a particular size plot low, and higher spatial densities plot toward the top; unity represents theoretical saturation and the horizontal line labelled “empirical saturation” is roughly the maximum practical density recognized in heavily cratered terrains of the surfaces of many planets and satellites (cf. Hartman 1984). In Fig. 2, we represent crater statistics by open symbols and boulders/PRFs by solid symbols.

III. CRATER POPULATION

Figure 1 presents frequencies for some of the larger craters on Eros. Shown for comparison are lines representing fits to crater data representing typical terrains from the higher resolution images of Gaspra, Ida, and Mathilde (Chapman *et al.* 1996b, 1996a, 1999). It is evident that the population of craters on Eros closely resembles the crater population on Ida, which has been interpreted to be in saturation equilibrium (or nearly

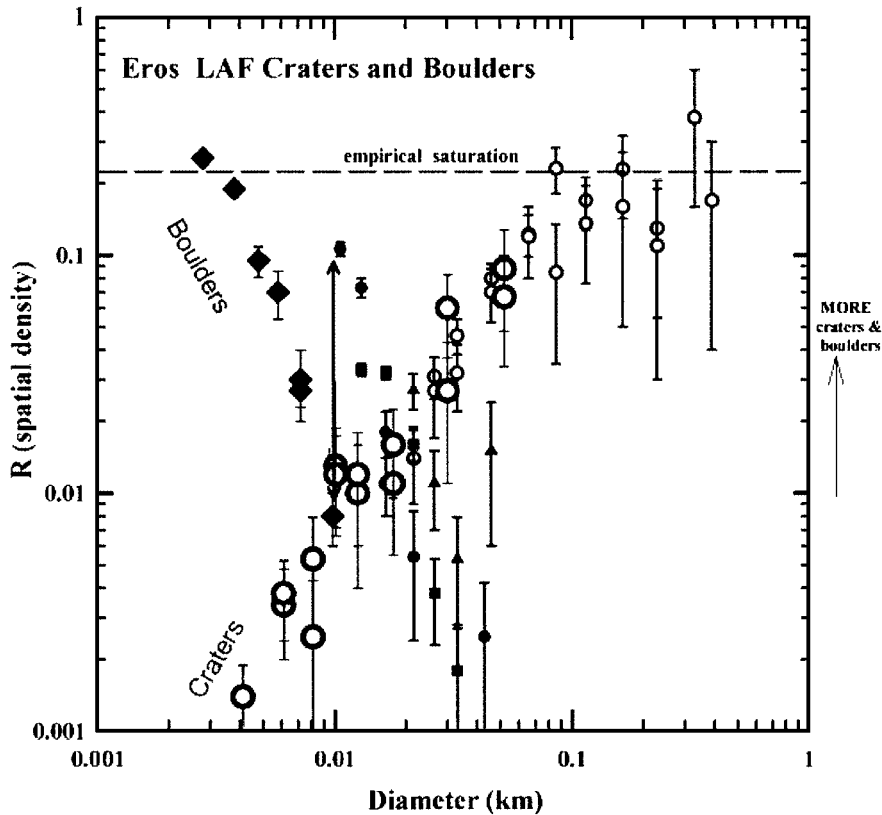


FIG. 2. This is an R-plot (see caption to Fig. 1) showing the spatial densities of boulders and of smaller craters on Eros, measured from relatively high-resolution images. In order to grasp the major trends, note that craters are indicated by open symbols, boulders by filled symbols. Larger symbols represent LAF data, smaller symbols are for data acquired from higher altitude orbits (some points also in Fig. 1). Different symbols represent different regions (see Table I). The vertical, double-headed arrow shows that boulder spatial densities are about 20 times *less* for the LAF region sample than for other regions studied.

so for some parts of Ida). The spatial density of larger craters on Eros is clearly greater than on Gaspra, where the production function has evidently not yet achieved equilibrium for craters with diameters >100 m.

Spatial densities of craters on Eros are not the same everywhere. The greatest differences are on the interior slopes of the largest features, like Psyche (the largest bowl-shaped impact crater on Eros) and Himeros (the largest topographic feature on Eros, a saddle-shaped concavity), where superimposed craters are uncommon, presumably affected by downslope mass wasting. We show some crater counts for a sparsely cratered portion of Shoemaker Regio (apparently a large, fresh, but irregularly shaped, impact crater) that are down from empirical saturation by about a factor of 10 near 200 m diameter. It is not yet clear whether such lower densities (in a locality having numerous large boulders) are due to the greater slopes or whether Shoemaker Regio is young and/or covered by boulders and ejecta from relatively recent impact/s in the vicinity. (The major features referred to in this article are shown in sketch maps accompanying other articles in this collection.)

Eros appears to be deficient in truly giant craters compared with Mathilde, which, unlike Eros, has a shape dominated by the numerous cavities comparable to the radius of the body. On the other hand, Eros is highly elongated and less equant than

Mathilde, so the largest crater (Psyche) and even larger possible impact features (Himeros and Shoemaker Regio), which are near the shorter axes of Eros, have roughly the size ratio relative to those axes that Mathilde's giant craters have to its diameter.

The cratering age of Ida has been estimated very roughly at ~ 2 Gyr (Chapman *et al.* 1996a); this highly model-dependent estimate derives from calculations of probable disruption time scales for rocky bodies of Ida's size combined with minimum estimates of how long it takes to saturate Ida with large craters, using an extrapolated size-distribution for small asteroids that would form such craters. Given that Eros shows a similar, saturated large-crater population and was presumably in a similar impact environment (although its precise former position in the main asteroid belt is unknown), we adopt a ~ 2 Gyr age for Eros—subject, of course, to all of the caveats about model dependency discussed by Chapman *et al.* (1996a, 1996b) in deriving approximate cratering ages for Gaspra and Ida. Eros must have acquired nearly all ($>99\%$) of its crater record while it was in the main belt, not during its recent, temporary, lifetime in Earth-approaching orbits (probably tens of Myr; see later discussion). Given theoretical understanding of the collisional cascade that generates the quasi-steady state size distribution of asteroids (cf. Durda *et al.* 1998), there has been every expectation that the size distribution of craters on asteroids would follow the empirical

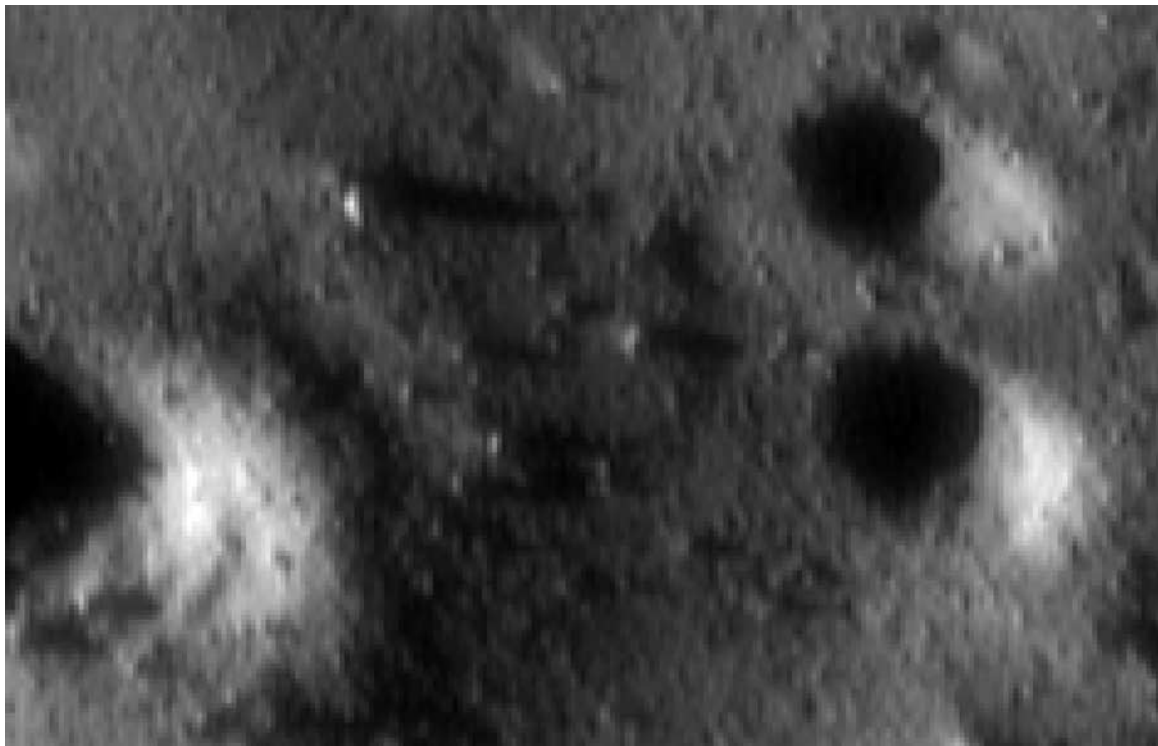


FIG. 3. Representative locality from part of a high-resolution low altitude flyover image (about 205 m by 154 m, resolution of about 1 m/pixel). Note lengthy shadows associated with some larger boulders; the boulder with the longest shadow is at lat/long = $-26.22/14.25$. Nearly all small-scale features are positive relief features (generally *not* showing long shadows), which form a surface that is generally “bumpy” near the resolution limit.

saturation line down to smaller sizes, as is observed, in the classic example, on lunar maria surfaces down to at least submeter size scales (Morris *et al.* 1968). This is not what we find, however.

At crater diameters <200 m and becoming prominent at diameters <50 m, the spatial density of craters drops off progressively relative to empirical saturation toward smaller sizes (Fig. 2). At least in the highest-resolution portions of the LAF imagery (cf. Fig. 3, which may or may not be representative of Eros as a whole), the spatial density of craters falls below empirical saturation by a factor of nearly 200 at a crater diameter of 4 m. On each LAF image, which may show many hundreds of boulders, only a few very small craters are visible (larger craters are more numerous), which differs qualitatively and dramatically from the appearance of the surfaces of the Moon or Deimos at equivalent resolutions. For example, in the Surveyor VI landing site in Sinus Medii (Morris *et al.* 1968), craters just 1 to 3 m in diameter have densities near the saturation equilibrium value. We discuss possible explanations for this surprising attribute of Eros later.

While we have not quantitatively studied the statistics of craters of different degradation states, a few qualitative observations are relevant. Moderate- and large-sized craters on Eros display the full range of degradation states from fairly fresh, bowl-shaped morphology down to barely recognized depressions, which is characteristic of the impact saturation equilibrium process with a “steep” production function. Preexisting

craters are eroded and degraded by subsequent saturation impacts of smaller projectiles and occasional blanketing by widespread ejecta from larger impacts; degradation may be enhanced by small-body-specific processes (which we amplify on below) such as net mass loss, more widely spread ejecta, and the enhanced role of seismic shaking. The net result of saturation equilibrium is a population dominated by moderately to highly degraded craters with a comparatively small fraction of fresh craters (cf. Chapman *et al.* 1970). The population of larger craters on Eros exhibits these traits.

At the smallest sizes (tens of m diameter and less), nearly all craters on Eros appear highly degraded with a very tiny percentage of fresh bowl-shaped examples. In this additional sense, the high-resolution appearance of Eros differs greatly from the moon, where fresh craters are recognized (although uncommon) down to very small sizes.

IV. BOULDERS

We have also assessed the size-frequency statistics for boulders and other PRFs in a few localities imaged from the 35 km and LAF orbits. As shown in Fig. 2, boulders larger than 50 m are extremely rare on Eros. The largest boulder identified to date is ~ 150 m across (Thomas *et al.* 2000), roughly agreeing with the prediction of Lee *et al.* (1996) based on a model of ejecta blocks excavated from the largest craters on a body. At diameters

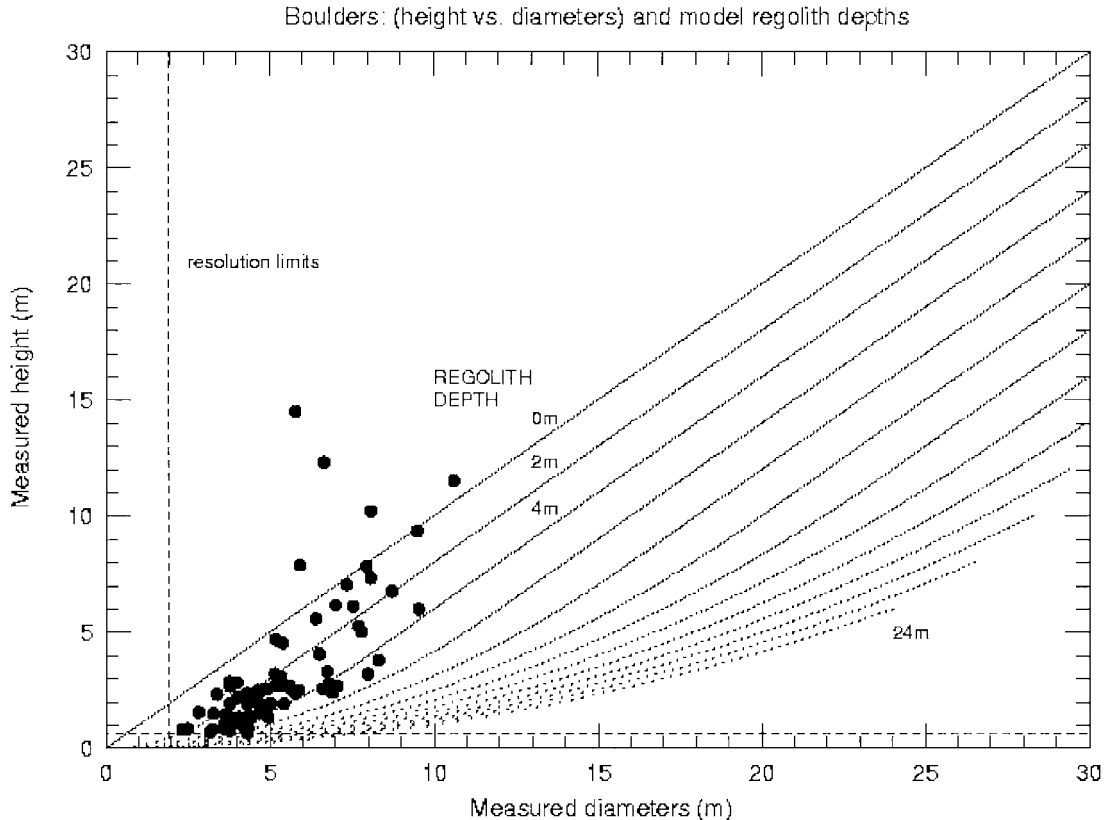


FIG. 4. Measurements of heights (determined from shadow lengths) vs. apparent diameter of boulders and positive relief features selected from in and near the locality shown in Fig. 3. Lines illustrate the depth of an idealized “regolith” computed on the assumption that boulders are spherical and resting on a hard substrate, with visible height and horizontal dimensions controlled by burial in a fluidized layer that reaches the indicated height. Small PRFs would be compatible with 2–3 m depth; larger boulders scatter widely (those above the 0 m line are taller than they are wide). If PRFs are nonspherical and lie in dynamically stable orientations then implied regolith depths would be correspondingly thinner.

<20 m, boulders start to become numerous; they roughly equal crater frequencies near 10 m in diameter. At still smaller sizes, PRFs greatly outnumber craters and, at the LAF resolution limit of ~ 2.5 m, exceed the empirical saturation line (which is relevant for craters; there is no reason that this line should similarly limit PRF densities, although it would be difficult for PRFs to greatly exceed $R = 1$).

We call the larger, ≥ 15 m PRFs “boulders” because they have the angular, quasi-round appearance of boulders on the Earth, the Moon, and the martian satellites. A surprising number of them on Eros appear to be perched high on the surface and, from favorable viewing angles, one can even see under some boulders, which overhang the small zone of contact with the surface. Most PRFs, however, are too small to have their shapes well resolved in even the highest resolution images. The very smallest features studied in the LAF images may well differ in character from the larger boulders in being less high relative to their horizontal dimensions (Fig. 4). Whether they are simply unresolved boulders, perhaps more deeply buried in a thin regolith, or indeed are mostly a different kind of feature from the larger presumed ejecta blocks, is not yet clear. A variety of PRF morphologies is evident in landing sequence images.

PRFs sampled in different localities vary widely in spatial density (vertical offsets in Fig. 2). Indeed, the LAF region, so heavily covered with small PRFs, is actually deficient in larger boulders by a factor ~ 20 compared with other regions studied from 35-km orbit images (double-headed arrow in Fig. 2). In all cases, the extremely steep slopes of the PRF size distributions are similar, having a differential power-law index ~ -5 , which is similar to or even steeper than the index found on other bodies for boulders and for secondary craters (formed by ejecta blocks on higher gravity bodies; Shoemaker 1965).

V. DISCUSSION OF SMALL-SCALE CHARACTER OF EROS

In this section, we address the chief ways for understanding the extraordinary differences between the small-scale surface structures of Eros and the Moon: the abundant boulders and the extremely depleted craters. While these might be due to separate causes, the explanation/s are plausibly related. With regard to the craters, we need to find a reason why small craters are not (are not) being formed in expected numbers *or* an explanation for how the craters, once formed, have been destroyed. With regard to the boulders, we need to explain how so many

have been created and how they have avoided being eroded and destroyed.

Depletion of Small Craters

There are three kinds of explanations for a depletion of small craters: (a) there is a depletion of small impactors, (b) small projectiles exist but are inhibited in producing small craters, or (c) small craters are produced but subsequently erased. We will consider these explanations in reverse order.

Crater erasure. A widely accepted view is that a standard crater production function (due to the size distribution of projectiles) applies throughout the inner solar system (including the asteroid belt), having the form shown in Fig. 5 of Neukum and Ivanov (1994). The standard function formally spans lunar crater diameters from 10 m to 700 km, but Neukum and Ivanov describe extrapolations down to craters 1 m in diameter and even to microcraters. If we assume that craters on Eros must have been forming according to this distribution, whether in the main belt or since entering Earth-approaching orbit, then the observed depletion of small craters must be due to subsequent degradation and destruction of craters by some strongly size-dependent geological process. Given that the production function has a differential index of -4 in the size range where craters are depleted (Neukum and Ivanov 1994) and the observed small-crater population has an index of -1.5 , a steady state crater destructive process would have to be much more strongly size-dependent ($D^{-2.5}$) than applies to usual crater destructive processes (e.g., D^{-1} for simple filling; cf. Chapman 1974). A quasi-steady state process is indicated by the progressive decline in crater numbers; a single episode of strongly size-dependent crater destruction (e.g., blanketing by ejecta from one large impact) would tend to destroy all craters smaller than a certain size, leaving all of the larger ones, contrary to observation.

Several lunar and planetary processes commonly invoked to degrade craters and other topographic features seem to be incapable of explaining the observed crater depletion. The impact process itself destroys small craters; this is what operates on the lunar surface and results in a crater population following the empirical saturation curve, as had been expected for Eros but which we now find is dramatically contrary to observation. Episodic blanketing by widely distributed cratering ejecta, expected on a small body, would not have such strongly size-dependent effects since it is essentially a filling process with a $1/D$ dependence; moreover, boulders would be blanketed, too. The usual endogenic geological processes, like volcanism and aeolian erosion/deposition, are difficult to imagine having ever operated on Eros.

One process that may be especially effective on small bodies like asteroids is seismic shaking (Hörz and Schall 1981). Any enhanced seismic response (“ringing”) of a small body in response to an impact combined with the much lower surface gravity could shake and erode topographic features. If smaller craters were preferentially formed in a mobile regolith, they might be destroyed much more rapidly than would larger craters

formed primarily in more competent material or bedrock. Seismically shaken regolith might be levitated, conceivably even onto escape trajectories; such responses would certainly erase craters formed in such a regolith. Such seismic shaking might also obliterate other indentations in the regolith, perhaps explaining the surprising rarity of boulder tracks and the depressions that should be made in the regolith surrounding boulders when they land. (Only a very tiny fraction of boulders are observed to be in dimples of their own making or at the ends of trails.) Progressive depletion of craters down to ~ 4 m in size would imply, in this scenario, that relatively small, frequent impacts—perhaps those that make craters only several hundred meters in size—cause Eros as a whole to “ring” violently. However, it is far from certain that Eros can be “rung” effectively at all: the difference between the bulk density of Eros compared with that of its presumed chondritic constituent material implies appreciable internal porosity, and the global lineament pattern on Eros shows that it has been heavily fractured (Wilkison *et al.* 2001), so efficient transmission of seismic shocks is questionable.

Inhibition of crater formation. The next logical branch of explanations for the scarcity of small craters is to suppose that few of them were formed in the first place despite the existence of small projectiles. F. Hörz (private communication 2000) has an explanation for a lack of small craters on the rock-littered Martian surface: he suggests that a small impactor striking a boulder, rather than a homogeneous semi-infinite surface, might expend its energy and momentum pulverizing the boulder and dispersing the resulting debris (as in an asteroid-asteroid collision) thus failing to form a crater in the boulder’s vicinity. Figures 2 and 3 suggest that Eros’ surface might be covered with discrete boulders < 10 m in diameter (in several regions on Eros) and < 3 m in diameter in the LAF region (landing sequence images, taken 12 February 2001, show large densities of boulders/rocks/PRFs of various sizes, but the surface—in this locale, at least—is obviously *not* armored by a large enough spatial density of boulders > 5 – 10 m in size to prevent cratering, as hypothesized). It is questionable if boulders < 10 m diameter could prevent the formation of craters 100 to 200 m in diameter, the sizes near which the observed depletion begins; it would require a target boulder to absorb the energy and momentum of a hypervelocity impactor up to twice its own size, which seems wholly unrealistic.

Paucity of small impactors. The easiest way to account for an absence of small craters is if there are very few projectiles in the cm to 10-m size range that form craters of the sizes where they are observed to be depleted. That is, perhaps the Neukum/Ivanov production function is wrong. Indeed Bell (2001) suggests that the Yarkovsky Effect (cf. Peterson 1976), which moves objects of just these sizes toward resonant escape hatches in the asteroid belt, might strongly deplete such objects. That it does, to some degree at least, is accepted as the predominant mode for delivery of meteorites from the asteroid belt to Earth (Vokrouhlický and Farinella 2000). (Yarkovsky forces are far less effective in size-sorting in near-Earth space because bodies of all sizes are

subject to dynamical loss processes on very short time scales; however, by enhancing delivery of meteorite-sized objects into near-Earth space compared with the slower, less efficient forces that extract larger objects, like Eros itself, from the asteroid belt, the Yarkovsky Effect actually accentuates the numbers of small projectiles striking, say, the Moon.)

The quantitative question is whether the effect is so strong that it would dominate over the repopulation of such bodies by the collisional disruptions and cratering of large asteroids. The required steady state depletion is very large. Numerical simulations of the collisional cascade combined with radiation forces (like the Yarkovsky Effect) are in their infancy (Vokrouhlický and Farinella 2000) so the final answer won't be known for a while. However, crude estimates can be made. If the Neukum/Ivanov curve is fitted to the larger craters on Eros, then we can estimate that the number of 4 and 30 m craters observed in the LAF region is a factor of $\sim 10^{-5}$ and $\sim 10^{-2.5}$, respectively, of the total number that would have been formed. Perhaps only the most recent third of those craters would have been formed since the last saturation of the surface by large craters. Thus, we would require a steady state depletion by a factor of $\sim 10^{-4.5}$ for the ~ 30 -cm-sized projectiles that make 4-m craters and a factor of $\sim 10^{-2}$ for the 2-m diameter projectiles that make 30-m diameter craters. Calculations of Yarkovsky drift rates for 2-m diameter rocky, fairly rapidly spinning meteoroids by Bottke *et al.* (2000) yield residence times in the main belt of belt of ~ 20 Myr, consistent with cosmic-ray exposure ages of many types of stony meteorites. Thus, Yarkovsky drift can deplete 2-m objects by a factor of $\sim 10^{-1.5}$, only a factor of 3 less than what is required. However, the observed depletion of small craters is a strong, $D^{-2.5}$, a function of crater size, whereas the size-dependency of Yarkovsky drift is only $\sim D^{-0.5}$ (Bottke *et al.* 2000). Thus, Yarkovsky drift fails to account for the depletion of the smaller 4-m craters by a factor of hundreds.

However, we can actually account for the depletion of craters >20 m diameter if we adopt the Dohnanyi (1971) equilibrium cascade production function, which is shallower (index -3.5) than that of Neukum/Ivanov. Indeed, this may be more relevant if the Neukum/Ivanov production function is artificially enhanced in near-Earth small particles due to supply from the asteroid belt by the Yarkovsky Effect. [The exact equilibrium production function will be affected over wide diameter ranges by the depletion itself, which can produce “waves,” (cf. Durda *et al.* 1998) so integrated numerical calculations are required.] But we are still short by a factor of about 30 in explaining the depletion of 4-m craters. Perhaps the alternative processes discussed earlier (e.g., armoring by boulders; seismic shaking) can contribute to further losses of craters <10 m diameter, even though we judged the processes to be inadequate to explain the entire depletion.

Abundance of Boulders and Other PRFs

Boulders on Eros were predicted (cf. Lee *et al.* 1996) by analogy with the Moon, martian satellites, and Ida, in which they are taken to be blocks ejected from the largest craters formed on those bodies. Widespread distribution of ejecta blocks might

be more common on a very low-gravity body than on the Moon or larger planet because low-velocity ejecta that would ordinarily wind up in continuous ejecta blankets or crater rims would travel much farther. Indeed, although quantitative statistics have not yet been tabulated, we observe that ejecta rims are generally much lower or absent on Eros compared with lunar craters. Furthermore, ejecta blocks (and secondary craters formed by them) are known to follow very steep size-distributions (index -4.5 or -5), at least down to sizes 10% of the size of the largest ones, just as observed for PRFs on Eros. In this connection, however, we should be cautious about associating such ejecta blocks and secondary craters observed on lunar and planetary surfaces with dispersed crater rim materials on asteroids since the materials are derived from very different locations during the excavation stage of cratering (Melosh 1989, ch. 6).

While the uncommon largest boulders on Eros generally have the irregular, craggy morphology of discrete, strong, (although often fractured) blocks of rock, image resolution is inadequate to see the morphology of the smallest PRFs a few meters in size. There is some indication that the smaller features are shallower than their larger counterparts, as if they were either horizontally flat objects or else roughly equidimensional objects substantially buried in the regolith (Fig. 4). The large boulders, on the other hand, are sometimes nearly as tall as they are wide, as though they had landed on a solid substrate with minimal penetration of, or subsequent covering by, a regolith. Occasionally, and surprisingly, some large PRFs are even taller than they are wide—a rather unstable orientation—suggesting that they may be slabs of bedrock sticking up from below.

The smallest PRFs cover a significant fraction of the surface in the LAF region studied, producing a “bumpy” character totally unlike the regolith surfaces of the Moon and Deimos (Fig. 3). We consider two plausible interpretations of this attribute of the surface (which was only marginally resolved in the images analyzed here and may be subject to artifacts): (a) exposure of a heavily fractured and bouldery bedrock with minimal or locally absent regolith, and (b) an ancient megaregolith dominated by multimeter scale blocks from the largest impacts, with a modest fraction of finer regolith materials. In either case, we consider any traditional regolith of pebbly/sandy/dusty fines to be a volumetrically much smaller portion of surface materials; at a minimum, they might account for deposits with an average depth of only the order of 1 m, which occasionally collect into the thicker, flat deposits in topographic lows called “ponds” (Veverka *et al.* 2001). It is unknown what process makes such units so flat, with such sharp edges—possibly seismic shaking or transport of electrostatically levitated dust, but no detailed models have yet been developed.

Heavily fractured bedrock. There are unconfirmed hints of regularity in the spatial distribution of the smaller PRFs (and even of some of the larger boulders). The flatter, more horizontal morphology of smaller PRFs (Fig. 4) may imply that they are fundamentally different from the larger, often perched blocks; perhaps they are exposures of fractured bedrock; but, alternatively, it may simply be that normal ejecta blocks are

more completely buried in a thin regolith. A few of the exceptionally tall larger boulders seem to have elongated, fin-like shapes—oriented in directions consistent with the global lineament pattern—which might also be explained as elements of *in situ* structure rather than randomly deposited ejecta blocks (Cheng *et al.* 2001a). Quantitative statistical analysis of feature elongations and alignments has not yet been done; care must be taken to correct for systematic effects associated with illumination angle, directionally oriented slopes on which features sit and their shadows are cast, MSI's rectangular pixels, etc. The highest resolution images, taken near the periphery of Himeros during the landing sequence, show no evidence for pervasive exposure of intact structure.

Megaregolith of ejecta blocks. Should the apparent alignments of PRF directionalities with the global fabric prove to be illusory and the PRFs turn out to have random shapes and locations, then the preferred interpretation would be as a megaregolith of ejecta blocks. The formation of Psyche hundreds of Myr ago would have covered Eros with the order of 10 m of ejecta blocks, depending on factors such as volumetric fraction

of blocks produced, fractional escape from the gravity field, and uniformity of distribution around Eros. If Himeros and Shoemaker Regio are also of impact origin, a layer up to several times that deep could have been deposited, depending on the same factors. A megaregolith of such ejecta could hardly be deeper; if it is found to be deeper, then it must reflect processes on Eros, or more likely its parent body, that predate the oldest observable features on Eros. Provided that only a small volumetric fraction of such a megaregolith were composed of finer materials, the resulting surface might be extraordinarily rough (like aa lava, as found by Cheng *et al.* (2001b) from fractal analysis of NLR LAF data) and could be visualized as a jumble of objects the sizes of busses, rooms, and trucks. While such a deposit transported from distant impacts could be technically termed a type of “regolith,” it would differ dramatically in nature from the more familiar, fine-grained, mature lunar regolith, which is developed largely by repetitive churning and comminution of basement rock derived *in situ*.

Figure 5 shows a fairly representative portion of the landing region at very high resolution, the fifth last image. (The last three images appear to be of an anomalously flat tract, possibly

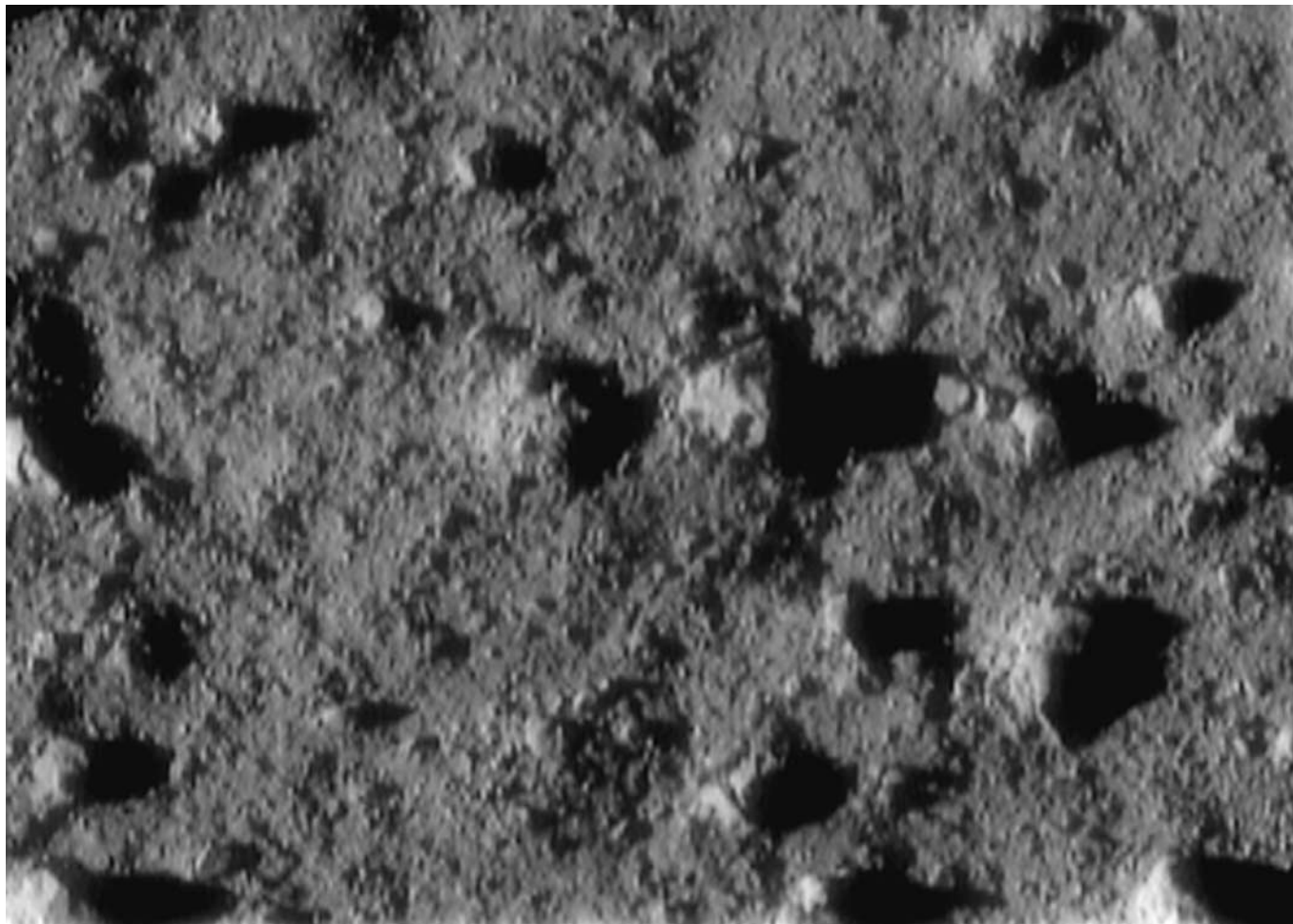


FIG. 5. The fifth last image taken during NEAR Shoemaker's landing sequence on 12 February 2001. The image shows a patch of rocky, rough terrain roughly 18 m across; illumination is from the left. The largest blocks are 2 to 3 m in size.

a “pond,” comparatively free of PRFs.) This image shows a very rocky, bouldery terrain, yet not quite at the aa lava extreme. It is, however, radically more rocky (immaturely comminuted) than the lunar surface at the same resolution.

Another puzzle about the PRFs is why, once created on Eros, they aren’t eroded into rounded shapes and subsequently destroyed by hypervelocity impact of small projectiles, which is what is believed to limit the lifetimes of boulders on the surface of the Moon. Some processes that might help explain the loss of small craters would also remove observable boulders (e.g., blanketing by thick ejecta would not only fill in craters but also cover over boulders of similar vertical dimensions). Conceivably such losses could be compensated for and overwhelmed by very efficient creation of new boulders (either by continuing exhumation of underlying fractured bedrock or as ejecta from recent craters).

Consistency of Explanations

Some of the explanations advanced independently for craters and boulders are self consistent while others may not be (for example, we have just noted that passive blanketing that might fill in small craters would also cover over boulders). The most compatible explanations are those in which (a) craters are destroyed by processes that don’t destroy boulders or (b) the impacting projectiles that would erode and destroy boulders are absent and thus also fail to form craters. Also, if there were somehow an unlimited resupply of boulders from a deep layer of megafragments or bedrock, then a process such as erosion could destroy both craters and boulders but only the craters would remain depleted. Several scenarios may meet these requirements, which we describe in what we judge to be decreasing order of plausible importance (all suffer from unresolved issues).

Few small projectiles. The most obvious idea is an absence of small projectiles, as hypothesized by Bell (2001): if small projectiles are strongly depleted, few small craters are formed and existing boulders remain pristine and uneroded. Quantitative verification of the idea depends on yet-to-be-done simulations of the collisional cascade in the presence of Yarkovsky forces. However, as described above, Yarkovsky depletion appears to work for craters 20–30 m in diameter if the Dohnanyi (1971) collisional equilibrium size distribution applies; other processes (like those below) would have to augment the Yarkovsky effect to explain depletion of smaller (e.g., 4-m) craters.

Seismic shaking. Shaking might efficiently degrade/destroy small craters in any loose regolith that exists while leaving strong, cohesive boulders intact. Indeed, the numbers of boulders at the regolith surface might be enhanced by jostling up from below (Hörz and Schall 1981; see also Asphaug *et al.* 2001). However, seismic shaking would also tend to move boulders downhill, leaving tracks in the regolith and concentrating boulders at topographic lows; such tracks and concentrations are rare. (Though shaking would also remove tracks, just as it removes craters, that wouldn’t happen until the next major impact.) If the seismic shaking were strong enough to actually launch ejecta into space, then boulders might also be depleted in that way.

Blocky surface (bedrock or deep, blocky megaregolith). As previously described, such a surface of blocks of bedrock or megaregolith might help armor the surface from small-crater formation. While the process also results in destruction of blocks, there could be a resupply of blocks from below *provided* that the debris from the destroyed blocks doesn’t form a regolith that blankets the blocks (e.g., if debris were ejected at greater than escape velocity, which is conceivable for small impacts into coherent rock; cf. Giblin *et al.* 1994). However, any residual regolith accumulation might “run away,” as it lowered subsequent ejecta velocities; it would then form a traditional regolith in which craters could form, contrary to observation. Previous studies (e.g., Housen 1992) have suggested that the transitional asteroid size between one that loses ejecta and one that substantially retains ejecta is much smaller than Eros, but the idea should be reexamined. End-of-mission imaging by NEAR Shoemaker has revealed that the surface is, in fact, blocky, but, as we noted above, not blocky enough to armor the surface from formation of 100-m scale craters; whether this location in the vicinity of Himeros is representative of other areas on Eros is unknown. We previously noted that such protection-by-blocks is energetically unrealistic except for playing a contributing role in depleting the smallest craters. Possible evidence that blocks partly inhibit formation of the smallest craters is found in images of nearly boulder-free ponds taken during the 28 January 2001 LAF, which appear to show more impact craters than on adjacent blocky terrains that are stratigraphically older than the ponds.

Summary: preferred explanation. In summary, the best explanation for pervasive boulders and few craters in high-resolution views of Eros is a depletion of small objects in the asteroid belt (Yarkovsky Effect; Bell 2001), probably augmented at the smallest scales by armoring of the surface from cratering by the numerous rocks and by topographic degradation by seismic shaking. Note that we explicitly disagree with the view of Veverka *et al.* (2001) that the paucity of craters is due to very effective “covering and erosion” of small craters by ejecta blanketing; we have noted above numerous reasons why this view is not tenable (the size-dependency expected for blanketing is too weak, blanketing would cover boulders as well as craters, etc.). The beauty of the Yarkovsky explanation is that the absence of small projectiles both extends the lifetimes of boulders and results in few craters; moreover, it operates in the asteroid belt but not on the Moon or Deimos, which indeed look different from Eros.

VI. CRATERING HISTORY OF EROS

We cannot deterministically trace the past orbital history of Eros because of chaotic dynamics. Presently, Eros’ aphelion distance of 1.78 AU restricts it from collisionally interacting with almost any main-belt asteroid, except those few with high eccentricities near the belt’s inner edge. But Eros’ orbit has surely undergone major variations since Eros left the asteroid belt. Numerical simulations of the dynamics over 5 Myr of 16 Eros

clones (fictitious bodies with orbital elements different from Eros itself by small deltas) by Michel *et al.* (1998) illustrate the most likely orbital behaviors for Eros. In particular, Eros' orbital behavior is of an unusually long-lived character for a near earth asteroid (NEA), but Eros still has a *much* shorter past (and future) lifetime than the age of the solar system. Michel *et al.* also addressed, in advance of NEAR Shoemaker's arrival at Eros, the possible impact history of Eros.

Let us consider the plausible collisional and dynamical history of Eros, paying special attention to the implied observable cratering history. First, as stated earlier, saturation cratering of Eros (diameters >200 m) must have occurred almost entirely *in the asteroid belt*, not since it has been in Earth-approaching orbits. Moreover, it must have been exposed to cratering, subsequent to its "creation" by catastrophic fragmentation of a parent body, for a much longer time (we have adopted 2 Gyr) than the ~200 Myr cratering age estimated for undersaturated Gaspra (Chapman *et al.* 1996b). It was during this time that nearly all of the larger geological structures (e.g., large craters and grooves) developed their degraded, softened appearance, presumably by some combination of subsequent smaller impacts, blanketing by ejecta from the largest impacts, seismic shaking, etc.

Creation of Eros by parent-body break-up presents an issue. If, as interpreted by Veverka *et al.* (2000) and Zuber *et al.* (2000), the global lineament pattern on Eros implies retention of planes of weakness ("fabric") inherited from its precursor body, then the parent-body break-up must have produced differential accelerations across the 34-km length of Eros that were insufficient to disassemble the object, which was presumably composed of rock already internally fractured during the object's previous impact shock history. It is reasonable to assume that only the largest, most centrally located "core" fragments of the parent body could survive with inherent structures largely intact. Eros probably is such a remnant parent-body core and is unlikely to have been an exterior fragment. Thus, no side of Eros would be expected to have ever had, or retained, surficial geological structures—such as craters—predating break-up of the body. So while the fabric of the parent body may be retained by Eros, all other surface features are presumed to have formed since Eros became an independent body.

Zappalà *et al.* (1997) proposed that the catastrophic break-up of a sizeable parent asteroid that created the Maria family might be the origin for the large near-Earth asteroids Eros and Ganymed. In their scenario, however, Eros would have been placed in the 3 : 1 resonance immediately and begun its orbital evolution quickly. Indeed, it probably would have evolved in a few million years to crash into the Sun (90% die within 11 Myr, as discussed by Gladman *et al.* 1997, and Migliorini *et al.* 1998). Such quick evolution seems to be incompatible with the very long times expected between such major family-producing collisions. If we were so extremely lucky enough that the Maria family formed less than a few tens of Myr ago so that we can be observing Eros during its brief history as an Earth-approacher, we would not expect it to be heavily cratered at all.

The numerical simulation of the dynamics of 16 Eros clones by Michel *et al.* (1998) presents a very different picture of Eros' likely origin. As noted above, Eros is in a type of orbit that is unusually long-lived for NEAs, with a typical lifetime of 50–100 Myr before solar crash, ejection from the solar system by Jupiter, or less likely impacts with the terrestrial planets. Rather than being derived from the immediate vicinity of a resonance, objects such as Eros are likely derived from more typical parts of the belt; following creation by parent body disruption, they slowly diffuse (due to numerous minor resonances) to become Mars-crossing (Migliorini *et al.* 1998). Thus, Eros is expected by Michel *et al.* to have been formed "long before its eventual insertion into the current Mars-crossing orbit." Though nearly all of its cratering occurred *before* it became Mars-crossing, there is the possibility that its orbital aphelion generally continued to remain in the asteroid belt (although not right now), in which case it might have continued to be cratered at the same rate during the last several tens of Myr, accounting for a few percent of its craters at most.

Michel *et al.* (1998) have calculated the average intrinsic collision probabilities with main-belt asteroids of their 16 clones and also the mean impact velocities. They find that individual clones range from having impact histories comparable to that of an average main-belt asteroid (3 of the 16 clones) to having cratering rates down by two orders of magnitude (half of the clones).

Perhaps, like half the clones, the cratering rate on Eros has been depressed by a factor of ~100 during the last many tens of Myr, a cratering hiatus. For example, if Eros formed ~2 Gyr ago and has been decoupled from main-belt cratering for 50 Myr, then it has received only 0.025% of its cumulative cratering during the last 50 Myr. Recratering of Eros in near-Earth space, where the size distribution of small asteroidal projectiles has been well calibrated from studies of the largest Earth-impacting bolides and from Spacewatch (and other) surveys of the smallest NEAs, would begin to appear as an upturn in the small-crater size frequency relation only for craters <10 m. Such an upturn is not seen in Fig. 2, with a shortage of 4-m diameter craters of at least a factor of 10; craters several centimeters to tens of centimeters in size seem, at first glance, to be very rare in the particular locality imaged during the landing sequence. If verified by quantitative measurements, this appearance suggests either that Eros has been out of the asteroid belt for a comparatively short time or that ongoing processes rapidly erase these tiny craters.

VII. THE S-TYPE CONUNDRUM AND SPACE WEATHERING

Background: S-Type Conundrum and NEAR's Compositional Measurements

One of the longest standing issues in asteroid science has been the nature of S-types, the second most common type of asteroid, and their relationship to meteorites. It has been debated whether (a) meteorites are a highly selective, nonrepresentative sample

of inner-main-belt asteroids and that spectral dissimilarities between S-types and ordinary chondrites (OCs) mean that S-type asteroids are parents of rare or nonsampled meteorites (e.g., differentiated stony-irons, primitive achondrites) *or* (b) the sampling is roughly representative and the spectral dissimilarities mean that nondifferentiated asteroidal surfaces are subject to some kind of “space weathering” process¹ that modifies OCs to appear S-like.

The pendulum has swung to favor the second option: that some or many S-types are space-weathered OCs. The evidence includes spatial variations in the reflectance spectrum of Ida (Chapman 1996), systematics of spectral data of Earth-approaching S-types (Binzel *et al.* 1996), and laboratory simulations of plausible space weathering processes (Moroz *et al.* 1996; Yamada *et al.* 1999; Sasaki *et al.* 2001). But the arguments have remained indirect and debatable. NEAR Shoemaker’s complementary instruments (X-ray, γ -ray, near-IR spectroscopy, and multispectral imaging, plus additional constraints on bulk density and central condensation from radio science and laser-ranging) were designed to address composition more comprehensively, with unprecedented mapping coverage and high resolution. Compositional variations across the surface of an asteroid can be especially diagnostic, as first shown by Gaffey (1984) from spectral differences resolved only hemispherically; Chapman (1996) later studied compositional variations on Ida at Galileo’s much higher resolution.

Of course, Eros is only a single example of the very large and heterogeneous S-type class and NEAR’s results cannot be blithely applied to all other S-types. However, Eros is a good test of inferences from ground-based studies. While Eros appeared to be in the S(IV) subclass of Gaffey *et al.* (1993), considered to be more likely (or least unlikely) to be OCs than any other S-type subclass, reinterpretation of old Eros spectra by Murchie and Pieters (1996) revealed possible hemispheric variations that, although small, were greater than would be expected for a homogeneous, nondifferentiated parent body.

Now that NEAR’s mission has ended, a picture of Eros’ mineralogy has emerged. Its evident spatial homogeneity in spectral properties, as observed by both the near-infrared spectrometer (NIS) and especially by the multispectral imager (MSI) (Veverka *et al.* 2000), as well as preliminary chemical data from the X-ray detector (thanks to energetic solar flares accompanying solar maximum; Trombka *et al.* 2000) both point *away* from any differentiated composition and *toward* an OC composition. The combined data sets permit only L or LL chondrites as an

analog for Eros among known meteoritic assemblages (McCoy *et al.* 2001), provided that a possible deficiency of sulfur is due to volatilization by micrometeoritic impact rather than partial differentiation of the whole body. The OC interpretation for the composition of Eros is consistent with its 2.67 g/cm³ bulk density (Yeomans *et al.* 2000) and with preliminary evidence that the density is homogeneous, given L- or LL-like densities and a modest fraction of void space.

Spatial Color Uniformity: Comparison of Ida and Eros

Accepting that Eros is an L- or LL-like assemblage, there remains a striking puzzle. To date, the NIS and MSI color/spectral data indicate very modest (a few percent, at most) color variations across the surface of Eros (Veverka *et al.* 2000). None of it is attributable to intrinsic mineralogical differences. Some differences may be photometric effects; there are also slight correlations with geology [especially steep slopes and high albedo units, perhaps related to slight freshening competing with space weathering (Clark *et al.* 2001)]. This extraordinary spectral uniformity extends down to the best resolutions achieved by NIS before it went out of service in May 2000 and even to the scale of boulders resolved during LAF color imaging (Veverka *et al.* 2001).

Such spatial uniformity, however, was not expected on the basis of earlier observations of Eros or the experience of Ida. The small hemispheric color differences interpreted from ground-based data for Eros (Murchie and Pieters 1996) turned out not to be real, apparently dominated by systematic errors. The tens-of-percent color variations on Ida were reasonably interpreted (Chapman 1996) in terms of an OC body subject both to space weathering and impacts, which would seem to apply to Eros. Recent impacts would excavate fresh OC material (with spectral traits approaching OC), which would then be gradually space-weathered into S-type (reddened) colors. Why is this not observed on Eros? If Eros is truly of OC composition, then its S-type (rather than OC-like) colors must reflect some generic space weathering; but where is the fresher material?

Ida rather than Gaspra is the better analog for Eros, because Galileo’s observations of Ida were more comprehensive, and at better resolution. Moreover, Gaspra is geologically and spectrally dissimilar from Eros: it has a low crater density and its spectrum is too olivine-rich to be OC. Indeed, Chapman (1997) concluded that Gaspra is probably a metal-rich, differentiated body. But Ida, like Eros, is an S(IV) with a similar bulk density and an apparent OC composition. Major color variations across Ida have been modeled (Geissler *et al.* 1996) as ejecta from the largest (~7 km diameter) recent impact crater on Ida, Azzurra. Spectra of both Azzurra and its irregularly distributed ejecta are much more OC-like than most of Ida (Chapman 1996); Sullivan *et al.* (1996) and Chapman (1996) also noted other small, fresh craters with more OC-like spectra. Hence, recent impacts on Ida penetrated the surficial regolith to bedrock, excavated OC-like materials, and ballistically distributed those materials in

¹ “Space weathering,” as used in this article, refers to the suite of processes (known and unknown) that modifies the optical reflectance properties (especially spectral reflectance) of surface materials with time. That such spectral changes with time *happen* has long been well-documented for the Moon, and more recently for asteroids. While the process(es) are believed to be due to exposure of the surface materials to space, and hypotheses of specific processes have been proposed, the details of *what* causes space weathering is of less concern in this discussion so long as it occurs for bodies in near-Mars and near-Earth space.

patches around the body; they have not had time to reach spectral maturity.

Azzurra's age is uncertain. It is the sixth or seventh largest crater recognized on Ida and may be the morphologically freshest. Indeed, it may be fresher than any crater on Ida's well-imaged side down to 1.5 to 2 km diameter. Although Azzurra *could* have formed very recently, its likely age is ~ 100 Myr, a small fraction of Ida's ~ 2 Gyr age. Less than 5% of prominent, small craters on Ida's well-imaged side exhibit immature colors, again implying a time scale for space weathering $\sim <100$ Myr.

Why Eros Is Bland: Space Weathering Has Gone to Completion

Macroscopic cratering operates much faster in the main asteroid belt than interior to the belt where rates are down by 2 to 3 orders of magnitude. It is virtually certain that no Azzurra-like crater could have formed on Eros since it left the main asteroid belt. Indeed, the largest crater expected to have been formed on Eros during the last 50 Myr would be only a couple of hundred meters in diameter, which—depending on where it formed and the depth of any regolith or ejecta layer—might well fail to penetrate to, and excavate, bedrock. Or, if it did penetrate to bedrock, the widespread ejecta from such a small crater would be too thin to opaquely cover the surface all around Eros, thus explaining the lack of freshly excavated materials like those observed on Ida.

We suggest, therefore, that all geological units resolvable on Eros by NEAR spectral instruments have had a chance to spectrally mature, or nearly so, under space weathering during the time Eros has been decoupled from cratering at main-belt rates. If such a virtual hiatus in large-scale cratering happened and was long enough, it would explain Eros' spectral uniformity. While "space weathering" is a generic term not implicating any particular physical process for modifying the spectral properties of asteroidal bedrock to S-type characteristics, several physical mechanisms have been suggested. The most promising is instantaneous zapping of surficial grains by micrometeorites and, perhaps, by solar wind particles. Such processes ought to be widespread in the inner solar system, not restricted to the asteroid belt. Both comet dust and asteroidal dust spreads through interplanetary space due to radiation forces. Indeed, space weathering should be more efficient closer to the Sun, where there is a greater flux of solar wind particles and where impact velocities are higher. In the case of the Moon, the repetitive gardening of the lunar regolith due to the Moon's higher gravity and perhaps its inherent composition further augments lunar space weathering effects, which have long been held to be responsible for the extreme differences between laboratory spectra of returned lunar rock samples and regionally averaged spectra of the lunar surface.

Above we estimate that space weathering timescales on Ida are ~ 100 Myr. If the rate is several times more rapid for Eros, which is closer to the Sun and in a higher-velocity micrometeorite collisional environment, then it is plausible that the most recent excavations of fresh material just prior to Eros' orbital

removal from the main-belt collisional environment (if that indeed happened at least many tens of Myr ago) would have had time to become much more maturely space-weathered than have fresh features on Ida in the same duration; such time scales are compatible with those recently suggested as being physically realistic by Hapke (2000) and Sasaki *et al.* (2001).

A cratering hiatus on Eros thus may provide a natural explanation for what otherwise would seem to be an incompatibility between Eros and Ida, which are similar bodies in most respects other than spectral blandness. Quantification of these ideas may lead to better estimates of the relative rates of space weathering on Eros and Ida, which could even lead to clues about what the predominant space weathering process is. And it might lead to constraints on the type of dynamical orbit (among the classes defined by Milani *et al.* 1989 and discussed by Michel *et al.* 1998) that Eros has been in; that, in turn, might shed further light on Eros' place of origin within the main asteroid belt. In particular, this hypothesis seems to require (a) that Eros has indeed been decoupled from main-belt cratering and (b) that the duration of decoupling has been long enough for space weathering to mature, tens of Myr or longer. If these ideas are correct, then craters formed in the last few tens of Myr (a few craters >100 m in diameter globally plus more sub-10-m craters) should show immature colors; we have not yet examined the vast NEAR Shoemaker image set to verify if such features exist.

VIII. DISCUSSION AND CONCLUSIONS

We normally think of asteroids as being modified almost exclusively by ongoing collisions and cratering. Topographic features are created and destroyed in a quasi-steady-state fashion, occasionally spiked by the stochastic effects of a rare, large impact that may suddenly generate ejecta blankets, boulders, cracks, etc. If, however, Eros has been in a virtual hiatus in cratering activity for the last 1–5% of its existence, then we may be seeing a tableau of Eros as it existed tens of Myr ago. A corollary of such a hiatus is that other processes, which are normally overwhelmed by the usual cratering rates, become augmented in relative efficacy by two orders of magnitude. Such processes include, of course, space weathering, as discussed above. Other mass wasting, readjustment, and relaxation processes might also become manifest during a long cratering hiatus. For example, thermal cycling continues as Eros rotates every 5 h and the small expansions and contractions might yield accumulated downslope movement (thermal creep). If Eros has recently undergone polar wandering, as has been suggested due to its nearly identical b and c moments of inertia, changing magnitudes and directions of stress within the body might even yield observable tectonic features that would cross-cut virtually all impact craters. Electrostatic levitation of dust might result in net transport, perhaps creating some of the extremely flat "ponds" (depths of a few meters) observed in some topographic lows by imaging and NLR tracks during LAF (Veverka *et al.* 2001; Cheng *et al.* 2001a).

We have described several ways to explain the strong depletion of small impact craters on Eros, and the highly degraded morphologies of remaining craters. Enhanced endogenic geological processes during a cratering hiatus could augment such effects. A cratering hiatus might also help explain the prevalence of perched, craggy, uneroded boulders on Eros, in the following way. Conceivably, a small fraction of crater ejecta blocks wind up in temporary orbits around Eros, later leaking into heliocentric orbits or reimpacting the asteroid. In the usual situation, such reimpacts compete at a low level with the continued cratering of the surface by heliocentric projectiles and by low-velocity crater ejecta. However, during the hypothesized cratering hiatus, the decay and reimpact of blocks orbiting around Eros might continue for a while (depending on the time scale for decay) and could preferentially contribute to the population of blocks found on Eros; if they reimpacted during the hiatus, they would *not*, as might normally be the case, have been covered over, eroded, or destroyed by subsequent impacts and regolith evolution.

The primary surprise from high-resolution imaging of Eros is the remarkable depletion of small craters and the abundance of boulders and other PRFs. The predominant cause is likely to be that the asteroid belt is strongly depleted in projectiles of the sizes that would form such craters and destroy the boulders. In addition, the small size and low gravity of Eros compared with the Moon, which has been the benchmark for regolith studies, could result in dramatically different effects on Eros, such as widespread redistribution of ejecta and regolith (perhaps even loss to space), seismic shaking, and/or exposure of bedrock or megaregolith blocks from below.

ACKNOWLEDGMENTS

This research has been supported by the NEAR Shoemaker Project. We have benefitted from discussions with many other members of the NEAR Science Team as well as other colleagues. We thank Bob Strom and Paul Geissler for helpful reviews.

REFERENCES

- Asphaug, E., P. J. King, M. R. Swift, and M. R. Merrifield 2001. Brazil nuts on Eros: Size-sorting of asteroid regolith. *LPSC* **32**, 1708.
- Bell, J. F. 2001. Eros: A comprehensive model. *LPSC* **32**, 1964.
- Binzel, R. P., S. J. Bus, T. H. Burbine, and J. M. Sunshine 1996. Spectral properties of near-Earth asteroids: Evidence for sources of ordinary chondrite meteorites. *Science* **273**, 946–948.
- Bottke, W. F., Jr., D. P. Rubincam, and J. A. Burns 2000. Dynamical evolution of main belt meteoroids: Numerical simulations incorporating planetary perturbations and Yarkovsky thermal forces. *Icarus* **145**, 301–331.
- Chapman, C. R. 1974. Cratering on Mars. I. Cratering and obliteration history. *Icarus* **22**, 272–291.
- Chapman, C. R. 1996. S-type asteroids, ordinary chondrites, and space weathering: The evidence from Galileo's fly-bys of Gaspra and Ida. *Meteoritics Planet. Sci.* **31**, 699–725.
- Chapman, C. R. 1997. Gaspra and Ida: Implications of spacecraft reconnaissance for NEO issues. In *Near-Earth Objects: The United Nations Conference* (J. Remo, Ed.), *Ann. N.Y. Acad. Sci.* **822**, 227–235.
- Chapman, C. R., J. A. Mosher, and G. Simmons 1970. Lunar cratering and erosion from Orbiter 5 photographs. *J. Geophys. Res.* **75**, 1445–1466.
- Chapman, C. R., E. V. Ryan, W. J. Merline, G. Neukum, R. Wagner, P. C. Thomas, J. Veverka, and R. J. Sullivan 1996a. Cratering on Ida. *Icarus* **120**, 77–86.
- Chapman, C. R., J. Veverka, M. J. S. Belton, G. Neukum, and D. Morrison 1996b. Cratering on Gaspra. *Icarus* **120**, 231–245.
- Chapman, C. R., W. J. Merline, and P. Thomas 1999. Cratering on Mathilde. *Icarus* **140**, 28–33.
- Cheng, A. F., O. Barnouin-Jah, M. T. Zuber, J. Veverka, D. E. Smith, G. Neumann, M. Robinson, P. Thomas, J. B. Garvin, S. Murchie, C. Chapman, and L. Prockter 2001a. Laser altimetry of small-scale features on 433 Eros from NEAR-Shoemaker. *Science* **292**, 488–491.
- Cheng, A. F., O. S. Barnouin-Jha, M. T. Zuber, J. Veverka, D. E. Smith, G. A. Neumann, M. S. Robinson, P. C. Thomas, J. B. Garvin, S. L. Murchie, C. R. Chapman, and L. Prockter 2001b. Fractal analyses of small scale features on Eros. *LPSC* **32**, 2041.
- Clark, B. E., P. Helfenstein, J. F. Bell III, C. Peterson, J. Veverka, T. McConnachie, P. Lucey, S. L. Murchie, N. I. Izenberg, and C. R. Chapman 2001. Space weathering on Eros: Constraints from albedo and spectral measurements of Psyche crater. *Meteoritics Planet. Sci.*, in press.
- Crater Analysis Techniques Working Group (A. Woronow and 11 colleagues) 1979. Standard techniques for presentation and analysis of crater size frequency data. *Icarus* **37**, 467–474.
- Dohnanyi, J. S. 1971. Fragmentation and distribution of asteroids. In *Physical Studies of Minor Planets* (T. Gehrels, Ed.), *NASA Spec. Publ.* **267**, 263–295.
- Durda, D. D., R. Greenberg, and R. Jedicke 1998. Collisional models and scaling laws: A new interpretation of the shape of the main-belt asteroid size distribution. *Icarus* **135**, 431–440.
- Gaffey, M. J. 1984. Rotational spectral variations of asteroid (8) Flora: Implications for the nature of the S-type asteroids and for the parent bodies of the ordinary chondrites. *Icarus* **60**, 83–114.
- Gaffey, M. J., J. F. Bell, R. H. Brown, T. H. Burbine, J. L. Piatek, K. Reed, and D. A. Chaky 1993. Mineralogical variations within the S-type asteroid class. *Icarus* **106**, 573–602.
- Geissler, P., J.-M. Petit, D. D. Durda, R. Greenberg, W. Bottke, and M. Nolan 1996. Erosion and ejecta reaccretion on 243 Ida and its moon. *Icarus* **120**, 140–157.
- Giblin, I., G. Martelli, P. N. Smith, A. Cellino, M. DiMartino, V. Zappalà, P. Farinella, and P. Paolicchi 1994. Field fragmentation of macroscopic targets simulating asteroidal catastrophic collisions. *Icarus* **110**, 203–224.
- Gladman, B. J., F. Migliorini, A. Morbidelli, V. Zappalà, P. Michel, A. Cellino, Ch. Froeschlé, H. F. Levison, M. Bailey, and M. Duncan 1997. Dynamical lifetimes of objects injected into asteroid belt resonances. *Science* **277**, 197–201.
- Hapke, B. 2000. How to turn OC's into S's: Space weathering in the asteroid belt. *Lunar Planet. Sci.* **31**, 1087.
- Hartmann, W. K. 1984. Does crater "saturation equilibrium" occur in the Solar System? *Icarus* **60**, 56–74.
- Hörz, F., and R. B. Schaal 1981. Asteroidal agglutinate formation and implications for asteroidal surfaces. *Icarus* **46**, 337–353.
- Housen, K. R. 1992. Crater ejecta velocities for impacts on rocky bodies. *Lunar Planet. Sci.* **31**, 555–556.
- Lee, S. W., P. Thomas, and J. Veverka 1986. Phobos, Deimos and the Moon: Size and distribution of crater ejecta blocks. *Icarus* **68**, 77–86.
- Lee, P., J. Veverka, P. C. Thomas, P. Helfenstein, M. J. S. Belton, C. R. Chapman, R. Greeley, R. T. Pappalardo, R. Sullivan, and J. W. Head III 1996. Ejecta blocks on 243 Ida and on other asteroids. *Icarus* **120**, 87–105.
- McCoy, T. J., M. J. Gaffey, J. F. Bell III, W. V. Boynton, T. H. Burbine, C. R. Chapman, A. F. Cheng, B. E. Clark, P. E. Clark, L. G. Evans, P. Gorenstein,

- P. Lucey, L. McFadden, S. Murchie, L. R. Nittler, M. S. Robinson, S. W. Squyres, R. D. Starr, J. I. Trombka, and J. Veverka 2001. The composition of 433 Eros: A mineralogical-chemical synthesis. *LPSC* **32**, 1556.
- Melosh, H. J. 1989. *Impact Cratering: A Geologic Process*. Oxford Univ. Press, New York.
- Michel, P., P. Farinella, and Ch. Froeschlé 1998. Dynamics of Eros. *Astron. J.* **116**, 2023–2031.
- Migliorini, F., P. Michel, A. Morbidelli, D. Nesvorný, and V. Zappalà 1998. Origin of multikilometer Earth- and Mars-crossing asteroids: A quantitative simulation. *Science* **281**, 2022–2024.
- Milani, A., M. Carpino, G. Hahn, and A. M. Nobili 1989. Dynamics of planet-crossing asteroids: Classes of orbital behavior. *Icarus* **78**, 212–269.
- Moroz, L. V., A. V. Fisenko, L. F. Semjonova, C. M. Pieters, and N. N. Korotaeva 1996. Optical effects of regolith processes on S-asteroids as simulated by laser shots on ordinary chondrite and other mafic materials. *Icarus* **122**, 366–382.
- Morris, E. C., R. M. Batson, H. E. Holt, J. J. Rennilson, E. M. Shoemaker, and E. A. Whitaker 1968. III. Television observations from Surveyor VI. In *Surveyor VI Mission Report. Part II: Science Results*. J. P. L. Technical Report 32-1262, pp. 9–45.
- Murchie, S. L., and C. M. Pieters 1996. Spectral properties and rotational spectral heterogeneity of 433 Eros. *J. Geophys. Res.—Planets* **101**, 2201–2214.
- Neukum, G., and B. A. Ivanov 1994. Crater size distributions and impact probabilities on Earth from lunar, terrestrial-planet, and asteroid cratering data. In *Hazards Due to Comets and Asteroids* (T. Gehrels, Ed.), pp. 359–416. Univ. of Arizona Press, Tucson.
- Peterson, C. 1976. A source mechanism for meteorites controlled by the Yarkovsky effect. *Icarus* **29**, 91–111.
- Sasaki, S., K. Nakamura, Y. Hamabe, E. Kurahashi, and T. Hiroi 2001. Production of iron nanoparticles by laser irradiation in a simulation of lunar-like space weathering. *Nature* **410**, 555–557.
- Shoemaker, E. M. 1965. Preliminary analysis of the fine structure of the lunar surface. In *Ranger 7, Part 2, Experimenters' Analyses and Interpretations*. J. P. L. Technical Report 32-700, pp. 75–132.
- Sullivan, R., R. Greeley, R. Pappalardo, E. Asphaug, J. M. Moore, D. Morrison, M. J. S. Belton, M. Carr, C. R. Chapman, P. Geissler, R. Greenberg, J. Granahan, J. W. Head III, R. Kirk, A. McEwen, P. Lee, P. C. Thomas, and J. Veverka 1996. Geology of 243 Ida. *Icarus* **120**, 119–139.
- Thomas, P. C., J. Joseph, B. Carcich, J. Veverka, B. E. Clark, J. F. Bell III, A. W. Byrd, R. Chomko, M. Robinson, S. Murchie, L. Prockter, A. Cheng, N. Izenberg, M. Malin, C. Chapman, L. A. McFadden, R. Kirk, M. Gaffey, and P. G. Lucey 2002. Eros: Shape, topography, and slope processes. *Icarus* **155**, 18–37.
- Trombka, J. I., S. W. Squyres, J. Brückner, W. V. Boynton, R. C. Reddy, T. J. McCoy, P. Gorenstein, L. G. Evans, J. R. Arnold, R. D. Starr, L. R. Nittler, M. E. Murphy, I. Mikheeva, R. L. McNutt Jr., T. P. McClanahan, E. McCartney, J. O. Goldstein, R. E. Gold, S. R. Floyd, P. E. Clark, T. H. Burbine, J. S. Bhangoo, S. H. Bailey, and M. Petaev 2000. The elemental composition of Asteroid 433 Eros: Results of the NEAR-Shoemaker X-ray spectrometer. *Science* **289**, 2101–2105.
- Veverka, J., P. C. Thomas, J. F. Bell III, M. Bell, B. Carcich, B. Clark, A. Harch, J. Joseph, P. Martin, M. Robinson, S. Murchie, N. Izenberg, E. Hawkins, J. Warren, R. Farquhar, A. Cheng, D. Dunham, C. Chapman, W. J. Merline, L. McFadden, D. Wellnitz, M. Malin, W. M. Owen Jr., J. K. Miller, B. G. Williams, and D. K. Yeomans 1999. Imaging of Asteroid 433 Eros during NEAR's flyby reconnaissance. *Science* **285**, 562–564.
- Veverka, J., M. Robinson, P. Thomas, S. Murchie, J. F. Bell III, N. Izenberg, C. Chapman, A. Harch, M. Bell, B. Carcich, A. Cheng, B. Clark, D. Domingue, D. Dunham, R. Farquhar, M. J. Gaffey, E. Hawkins, J. Joseph, R. Kirk, H. Li, P. Lucey, M. Malin, P. Martin, L. McFadden, W. J. Merline, J. K. Miller, W. M. Owen Jr., C. Peterson, L. Prockter, J. Warren, D. Wellnitz, B. G. Williams, and D. K. Yeomans 2000. NEAR at Eros: Imaging and spectral results. *Science* **289**, 2088–2097.
- Veverka, J., P. C. Thomas, M. Robinson, S. Murchie, C. Chapman, M. Bell, A. Harch, W. J. Merline, J. F. Bell III, B. Bussey, B. Carcich, A. Cheng, B. Clark, D. Domingue, D. Dunham, R. Farquhar, M. J. Gaffey, E. Hawkins, N. Izenberg, J. Joseph, R. Kirk, H. Li, P. Lucey, M. Malin, L. McFadden, J. K. Miller, W. M. Owen Jr., C. Peterson, L. Prockter, J. Warren, D. Wellnitz, B. G. Williams, and D. K. Yeomans 2001. Imaging of small-scale features on 433 Eros from NEAR: Evidence for a complex regolith. *Science* **292**, 484–488.
- Vokrouhlický, D., and P. Farinella 2000. Efficient delivery of meteorites to the Earth from a wide range of asteroid parent bodies. *Nature* **407**, 606–608.
- Wilkison, S. L., M. S. Robinson, P. C. Thomas, J. Veverka, T. J. McCoy, S. L. Murchie, L. Prockter, and D. Yeomans 2001. The porosity of Eros and implications for its internal structure. *LPSC* **32**, 1721.
- Yamada, M., S. Sasaki, H. Nagahara, A. Fujiwara, S. Hasegawa, H. Yano, T. Hiroi, H. Ohashi, and H. Otake 1999. Simulation of space weathering of planet-forming materials: Nanosecond pulse laser irradiation and proton implantation on olivine and pyroxene samples. *Earth Planet. Space* **51**, 1255–1265.
- Yeomans, D. K., P. G. Antreasian, J.-P. Barriot, S. R. Chesley, D. W. Dunham, R. W. Farquhar, J. D. Giorgini, C. E. Helfrich, A. S. Konopliv, J. V. McAdams, J. K. Miller, W. M. Owen Jr., D. J. Scheeres, P. C. Thomas, J. Veverka, and B. G. Williams 2000. Radio science results during the NEAR-Shoemaker spacecraft rendezvous with Eros. *Science* **289**, 2085–2088.
- Zappalà, V., A. Cellino, M. DiMartino, F. Migliorini, and P. Paolicchi 1997. Maria's family: Physical structure and possible implications for the origin of giant NEAs. *Icarus* **129**, 1–20.
- Zuber, M. T., D. E. Smith, A. F. Cheng, J. B. Garvin, O. Aharonson, T. D. Cole, P. J. Dunn, Y. Guo, F. G. Lemoine, G. A. Neumann, D. D. Rowlands, and M. H. Torrence 2000. The shape of 433 Eros from the NEAR-Shoemaker laser rangefinder. *Science* **289**, 2097–2101.